

The Local Delay in Mobile Poisson Networks

Zhenhua Gong, *Student Member, IEEE* and Martin Haenggi, *Senior Member, IEEE*

Abstract—For communication between two neighboring nodes in wireless networks, the local delay, which is defined as the time it takes a node to successfully transmit a packet, is an important quantity. Previous research focuses on the local delay in static or infinitely mobile Poisson networks with ALOHA. In this paper, we extend the local delay results to Poisson networks with finite mobility. Bounds of the local delay in mobile Poisson networks are derived for different mobility and transmission models. Although mobility helps reduce the local delay, its impact depends on the particular mobility model. The phase transition that marks the jump of the local delay from finite to infinite is also characterized.

Index Terms—Interference, local delay, mobility, Poisson point process.

I. INTRODUCTION

A. Motivation

In a wireless network, it is fundamentally necessary that every node is able to successfully transmit messages to at least one other node in the network in a finite amount of time. Hence, the local delay, which is defined in [1], [2] as the average time (in numbers of time slots) until a packet is successfully transmitted, is an important quantity. The local delay and its phase transition condition in static Poisson networks are analyzed in [1]. The local delay in power- and interference-limited networks is presented in [2]. Only two extreme cases are considered in their analysis: the network is either completely static (nodes do not move after initial placement), or infinitely mobile (a new and independent Poisson point process (PPP) is drawn in each time slot). However, no work has analyzed the local delay under practical (finite) mobility models, which is the important intermediate regime between the two extreme cases. In this paper, we extend the local delay results to this practical regime. Each node has a randomly chosen initial (home) location and a mobility region. Due to the temporal correlation of the node locations and interference, the events of successful transmission are temporally correlated, which strongly affects the local delay. Mobility helps reduce the temporal correlation of the interference and outage in large wireless networks [3]. Here, we evaluate its impact on the local delay.

B. Related work

Besides the local delay analysis in static and infinitely mobile Poisson networks [1], [2], the local delay in clustered networks is analyzed in [4]. A set of power control policies

are provided in [5] to minimize the local delay in static Poisson networks. The interference correlation due to long transmission duration and the corresponding local delay are evaluated in [6] using joint interference statistics. The throughput/delay and power/delay tradeoffs for mobile ad hoc networks have been evaluated in [7], [8] and [9], respectively. A delay analysis for two-hop relay networks is presented in [10]. The delay in buffered ALOHA networks has been analytically characterized in [11].

Mobility models and their effects on the topology of ad hoc networks are compared in [12]. The benefits of mobility in wireless networks have been explored in terms of connectivity [13], [14], coverage [15], and capacity [16]. However, no work has analyzed the impact of node mobility on the local delay.

C. Main contributions

The main contributions of this paper are:

- 1) We calculate the local delay in mobile Poisson networks with concrete results or bounds for the local delay for deterministic, random static, and random time-variant transmission distances.
- 2) We evaluate the effects of mobility on the local delay under different mobility and transmission models.
- 3) We derive the range of network parameters under which a finite local delay can be achieved.

D. Paper organization

The rest of the paper is organized as follows. We introduce the system model in Section II. The local delay for deterministic transmission distance is presented in Section III. The local delay for random static transmission distance is discussed in Section IV. Section V presents the local delay for random time-variant transmission distance. Conclusions are drawn in Section VI.

II. SYSTEM MODEL

A. Transmitter process

The potential transmitters in a network are randomly distributed on \mathbb{R}^2 . Each of them has a home location and a mobility region. The home locations form a PPP $\tilde{\Phi} = \{y_i\} \subset \mathbb{R}^2$ with intensity λ . $\tilde{\Phi}$ is assumed temporally static. Nodes make an excursion in the mobility region independently of each other at each time $t \in \mathbb{Z}$ with a certain probability. The definition of the mobility models will be given in Section II-C. Hence at all times, the node locations form another PPP $\Phi_t = \{x_i(t)\} \subset \mathbb{R}^2$ (correlated with $\tilde{\Phi}$) with the same intensity λ . If a transmitter is scheduled to transmit at time t , we assume that the transmission starts at the beginning of that time slot. Each transmission is finished within one time slot. Slotted ALOHA with parameter $p > 0$ is assumed as the medium access control (MAC) protocol.

The authors are with the Wireless Institute, Department of Electrical Engineering, University of Notre Dame, Notre Dame, IN 46556, USA (e-mail: {zgong, mhaenggi}@nd.edu).

The support of the NSF (grants CNS 1016742 and CCF 1216407) is gratefully acknowledged.

B. Transmission scheme and receiver process

In Section III and IV, the receiver process does not affect the local delay calculation, since the transmission distance in the desired link is either deterministic or random static. In Section V, we consider three transmission schemes: random bipolar, quasi-nearest-receiver, and nearest-receiver models. Different transmission schemes lead to different local delays in the network.

1) *Random bipolar model*: We assume that each transmitter has an assigned receiver. The receivers are situated at the home locations of their assigned transmitters and stay fixed, *i.e.*, the receiver process is given by $\Psi = \tilde{\Phi}$. Those receivers can be thought of as randomly placed base stations. Each transmitter keeps transmitting to the same receiver. Figure 1(a) shows a realization of such a random bipolar network¹.

2) *Quasi-nearest-receiver model*: Here each transmitter conveys a message to a node that is close to the transmitter. We denote the receiver process as $\Psi = \{z_i\}$, which is a PPP with intensity λ' and independent of the transmitter process Φ_t . (Those nodes in Φ_t that are not scheduled to transmit are not available for reception.) Ψ is assumed temporally static. Each transmitter x_i chooses the receiver that is the closest to its home location $y_i \in \tilde{\Phi}$, *i.e.*, $z_i^* = \arg \min_{z \in \Psi} \{\|z - y_i\|\}$. We use the term “quasi-” to indicate that the receiver selected is not always the closest receiver to the transmitter’s current position. A realization of the Poisson network with quasi-nearest-receiver transmission is shown in Figure 1(b).

3) *Nearest-receiver model*: Different from the quasi-nearest-receiver model, where the receiver is chosen based on the distance to a transmitter’s home location, each transmitter $x_i(t)$ always picks the receiver that is the closest to it, *i.e.*, $z_i^*(t) = \arg \min_{z \in \Psi} \{\|z - x_i(t)\|\}$ under the nearest-receiver model. A realization of the Poisson network with nearest-receiver transmission is shown in Figure 1(c).

The validity of quasi-nearest-receiver and nearest-receiver models depends on the frequency with which the nodes exchange their location information. If every node exchanges its location with other nodes in each time slot t , we choose the nearest-receiver transmission scheme. If nodes do not (or seldom) exchange their location information, the quasi-nearest-receiver model is more appropriate. Hence, the difference between Figure 1(b) and 1(c) is that the transmitter keeps transmitting to the same receiver under the quasi-nearest-receiver scheme while it changes destinations in different time slots under the nearest-receiver scheme. Moreover, the transmission distance is not necessarily the shortest among all the potential receivers under the quasi-nearest-receiver scheme.

C. Mobility models

We use a constrained i.i.d. mobility (CIM) model, under which each node has a home location and makes excursions in a mobility region. Under CIM, the node locations in two different time slots are independent given the node’s home

¹The bipolar model usually has a fixed transmission distance (see Section 5.3 in [17]). In this model, however, the transmission distance is a random variable due to mobility.

location. We denote the pdf of the excursions by $f_w(x)$. Two specific models are considered.

Definition 1. *The node locations under the uniform mobility model (UMM) follow a uniform distribution in a ball of radius a_0 centered at the home location, *i.e.*,*

$$f_w(x) = \begin{cases} \frac{1}{\pi a_0^2} & \|x\| \leq a_0 \\ 0 & \text{otherwise,} \end{cases} \quad (1)$$

where $\|\cdot\|$ is the Euclidean distance.

The distance distribution between the home and the node locations is then given by

$$f_R(x) = \begin{cases} \frac{2x}{a_0^2} & x \leq a_0 \\ 0 & \text{otherwise.} \end{cases} \quad (2)$$

Definition 2. *The node locations under normal mobility model (NMM) follow a symmetric normal distribution with variance σ^2 centered at the home location, whose pdf is given by*

$$f_w(x) = \frac{1}{2\pi\sigma^2} \exp\left(-\frac{\|x\|^2}{2\sigma^2}\right). \quad (3)$$

The distance distribution is given by the Rayleigh distribution

$$f_R(x) = \frac{x}{\sigma^2} \exp\left(-\frac{x^2}{2\sigma^2}\right). \quad (4)$$

We define $v_i(t) \triangleq \|x_i(t) - x_i(t-1)\|$. Let

$$\bar{v}_i(t) \triangleq \mathbb{E}[v_i(t)], \quad \forall t \in \mathbb{Z}.$$

Due to ergodicity and point process homogeneity, the mean speed averaged over all nodes for a fixed time t is equal to the mean speed averaged over time for a fixed node. Hence, we drop i and t , and simply denote by \bar{v} the mean speed of the node. For UMM, we have $\bar{v} = 128a_0/45\pi$ [18, (8)] and for NMM, we obtain $\bar{v} = \sqrt{\pi}\sigma$. The mean speed \bar{v} is proportional to a_0 or σ .

The frequency at which nodes update their locations greatly affects the network geometry and performance. If nodes update their locations independently at time t with probability $1/K$, where $K > 1$, *i.e.*, $x_i(t) = y_i + w_i(t)$, where $w_i(t)$ is the random excursion, and stay at their previous locations with probability $1 - 1/K$, *i.e.*, $x_i(t) = x_i(t-1)$, we term this model *block mobility*. If the nodes update their locations in each time slot t , we then have $x_i(t) = y_i + w_i(t)$ (or $K = 1$ in the *block mobility* case). In order to distinguish the cases where $K > 1$ and $K = 1$, we term $K = 1$ *fast mobility*. In the analysis, the interfering transmitters are always assumed mobile. The desired transmitter is assumed static in Section III and IV, and assumed mobile in Section V.

D. Channel model and total interference

The attenuation in wireless channels is modeled as the product of a large-scale path-loss component and a small-scale fading component. The large-scale path-loss function is given by $\|x\|^{-\alpha}$, where α is the path loss exponent. For the multi-path fading, we consider Rayleigh fading with pdf $f_h(x) = \exp(-x)$, where $x \geq 0$. The Rayleigh fading

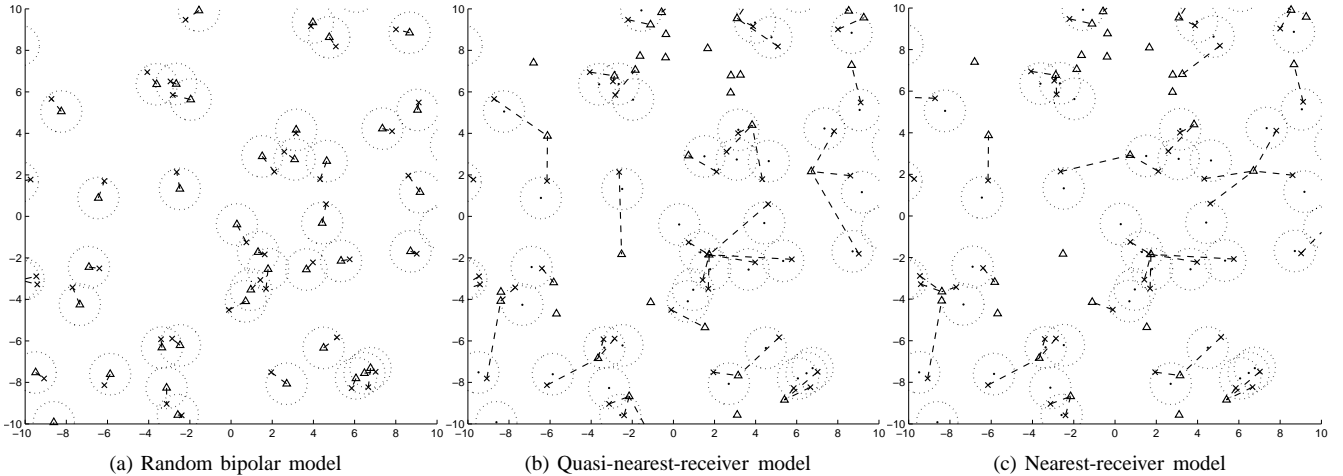


Figure 1: Illustration of the three transmission models. The triangles represent potential receivers (shortened as “receivers”), and the crosses represent potential transmitters (shortened as “transmitters”). The potential transmitter-receiver pairs are connected by dashed lines. The transmitters are mobile in a circular region of radius $a_0 = 1$. The dotted circles represent their mobility regions. The network intensity $\lambda = 0.1$. Under the random bipolar scheme (a), each transmitter has an assigned receiver, whose location is the home location of the transmitter. Under quasi-nearest-receiver (b) and nearest-receiver (c) schemes, the receiver process, whose intensity is $\lambda' = 0.07$, is independent of the transmitter process. In (b), the assigned receiver is not always the nearest receiver to the transmitter, and the transmitter keeps transmitting to the same receiver. In (c), however, the transmitter always transmits to its nearest receiver and thus changes destinations, if another receiver is closer. (See the middle part of (b) and (c) as an example.)

assumption is valid even if a node has no macroscopic mobility since multi-path fading is induced by slight changes in the location or environment.

At time t , the total interference at the receiver (located at z) is given by

$$I(t) = \sum_{x \in \Phi_t} T_x(t) h_x(t) \|x - z\|^{-\alpha}, \quad (5)$$

where $T_x(t)$ is i.i.d. Bernoulli with parameter p due to ALOHA and the multi-path fading $h_x(t)$ has mean $\mathbb{E}h = 1$. The random variables $I(t)$, $t \in \mathbb{Z}$, are exchangeable [19].

E. Local delay definition

Let \mathcal{S} be the static elements of a network. Assume the desired receiver² at the origin o , we let $\mathcal{C}_{\mathcal{S}}$ be the event that the receiver is successfully connected to its assigned transmitter in a single transmission conditioned on \mathcal{S} . The conditional success probability is given by

$$\mathbb{P}(\mathcal{C}_{\mathcal{S}}) = \mathbb{P}(\text{SIR} > \theta \mid \mathcal{S}),$$

where θ is a given threshold. If the receiver fails to decode a packet, it is retransmitted in the next scheduled transmission slot. Conditioned on \mathcal{S} , the success indicator random variables are temporally i.i.d. Hence, the distribution of the conditional local delay is geometric with mean $\mathbb{P}(\mathcal{C}_{\mathcal{S}})^{-1}$. The local delay is then the expectation with respect to (w.r.t.) \mathcal{S} :

$$D \triangleq \mathbb{E}_{\mathcal{S}} \left(\frac{1}{\mathbb{P}(\mathcal{C}_{\mathcal{S}})} \right). \quad (6)$$

D denotes the average number of slots that it takes the transmitter to successfully convey a packet to the receiver.

²In Section III and IV the origin o does not belong to the receiver process Ψ . In Section V, however, we need to slightly change the definition of the local delay.

III. LOCAL DELAY FOR DETERMINISTIC TRANSMISSION DISTANCE

In this section, we present some basic results on the local delay, which will be used in the following sections. For completeness, the conditional Laplace transform of $I(t)$ given \mathcal{S} in static networks ($\bar{v} = 0$) is given by

$$\mathcal{L}_0(s \mid \mathcal{S}) \triangleq \mathcal{L}_I(s \mid \mathcal{S} = \Phi) = \prod_{x \in \Phi} \left(1 - \frac{ps}{\|x\|^\alpha + s} \right), \quad (7)$$

whose derivation is presented in [2], and the unconditional Laplace transform of $I(t)$ in infinitely mobile networks ($\bar{v} = \infty$) is given by

$$\mathcal{L}_\infty(s) \triangleq \mathcal{L}_I(s \mid \mathcal{S} = \emptyset) = \exp \left(-\frac{\delta \lambda p \pi^2 s^\delta}{\sin(\pi \delta)} \right), \quad (8)$$

where $\delta \triangleq 2/\alpha$.

We assume that the transmission distance is R . The interfering transmitters are mobile following the mobility models introduced in Section II-C. Given R , we calculate the conditional local delay for the receiver at the origin. Two cases are considered: fast mobility and block mobility.

A. Fast mobility

If the excursions $w_i(t)$ are i.i.d. across time and space, the static elements of the network are $\mathcal{S} = \tilde{\Phi}$. We have the following proposition about the conditional Laplace transform of the interference and the conditional local delay.

Proposition 3. *Given the static elements of a network $\mathcal{S} = \tilde{\Phi}$, the conditional Laplace transform of the interference $\mathcal{L}_v(s \mid$*

\mathcal{S}) is given by³

$$\mathcal{L}_v(s|\mathcal{S}) \triangleq \mathcal{L}_I(s|\tilde{\Phi}) = \prod_{y \in \tilde{\Phi}} \left(1 - ps \int_{\mathbb{R}^2} \frac{f_w(x)}{\|y+x\|^\alpha + s} dx \right), \quad (9)$$

where $f_w(x)$ is the pdf of the excursion vector. Given a transmission distance R , the conditional local delay is given by

$$D_v(\theta | R) = \frac{1}{p} \exp \left(\lambda \int_{\mathbb{R}^2} \left(\frac{1}{1 - p\theta R^\alpha \int_{\mathbb{R}^2} \frac{f_w(x)}{\|y+x\|^\alpha + \theta R^\alpha} dx} - 1 \right) dy \right). \quad (10)$$

Proof: From (5), the total interference at the origin is given by

$$I(t) = \sum_{x \in \Phi_t} T_x(t) h_x(t) \|x\|^{-\alpha} = \sum_{y \in \tilde{\Phi}} T_y(t) h_y(t) \|y+w\|^{-\alpha}.$$

The conditional Laplace transform of the interference given $\tilde{\Phi}$ is thus given by

$$\begin{aligned} \mathcal{L}_I(s | \tilde{\Phi}) &= \mathbb{E} \left[e^{-sI(t)} | \tilde{\Phi} \right] \\ &\stackrel{(a)}{=} \mathbb{E} \left[\exp \left(-s \sum_{y \in \tilde{\Phi}} T_y h_y \|y+w\|^{-\alpha} \right) \middle| \tilde{\Phi} \right] \\ &\stackrel{(b)}{=} \exp \left(\sum_{y \in \tilde{\Phi}} \log \left(1 - ps \int_{\mathbb{R}^2} \frac{f_w(x)}{\|y+x\|^\alpha + s} dx \right) \right) \\ &= \prod_{y \in \tilde{\Phi}} \left(1 - ps \int_{\mathbb{R}^2} \frac{f_w(x)}{\|y+x\|^\alpha + s} dx \right), \end{aligned}$$

where (a) holds since the interferences $I(t)$ are exchangeable; (b) follows from [20, Lemma 16.6.5] and averaging over the random excursions. Furthermore, we have

$$D_v(\theta | R) \triangleq \mathbb{E}_{\tilde{\Phi}} \left(\frac{1}{p \mathcal{L}_I(s | \tilde{\Phi})} \right) \Big|_{s=\theta R^\alpha},$$

where the term $p \mathcal{L}_I(s | \tilde{\Phi})$ is the probability that the scheduled transmitter successfully transmits a packet. (10) is then imminent from (9) using the probability generating functional (pgfl) of the PPP. ■

The following corollary is then straightforward.

Corollary 4. *Given a transmission distance R , the local delay is lower bounded by*

$$D_v(\theta | R) \geq D_\infty(\theta | R).$$

Proof: From the definition of the local delay, we have

$$D_v(\theta | R) \stackrel{(a)}{\geq} \frac{1}{p \mathbb{E}_{\tilde{\Phi}} (\mathcal{L}_I(\theta | \tilde{\Phi}))} = \frac{1}{p \mathcal{L}_\infty(\theta)} = D_\infty(\theta | R), \quad (11)$$

where (a) holds due to Jensen's inequality. ■

³Similar to $\mathcal{L}_0(s|\mathcal{S})$ and $\mathcal{L}_\infty(s)$, the subscript v in $\mathcal{L}_v(s|\mathcal{S})$ indicates a mobile network, where the nodes are with finite mean speed.

The following proposition provides an upper bound of $D_v(\theta | R)$.

Proposition 5. *Let $a = a_0$ under UMM and $a = \sqrt{2}\sigma$ under NMM. The conditional local delay given a transmission distance R is upper bounded by*

$$D_v(\theta | R) \leq \begin{cases} \frac{1}{p} \exp \left(\frac{\lambda p \gamma a^2 R^2}{\pi a^2 - p \gamma R^2} \right) & a\beta > R \\ D_0(\theta | R) & \text{otherwise,} \end{cases} \quad (12)$$

where

$$D_0(\theta | R) = \frac{1}{p} \exp \left(\frac{\lambda p \gamma R^2}{q^{1-\delta}} \right), \quad (13)$$

$q = 1 - p$, and

$$\gamma \triangleq \frac{\delta \pi^2 \theta^\delta}{\sin(\pi \delta)} \quad (14)$$

is the spatial contention (see [2, (4)]), and $\beta \triangleq \sqrt{(1 - q^{1-\delta}) \pi / p \gamma}$.

Proof: See Appendix I. ■

$D_0(\theta | R)$ is identical to [2, (23)] and always finite for any given R and θ , so is $D_v(\theta | R)$. When $a \leq R\beta^{-1}$ ($a = a_0$ under UMM and $a = \sqrt{2}\sigma$ under NMM), we use $D_0(\theta | R)$ (the static case) to bound the local delay. If $a > R\beta^{-1}$, a tighter upper bound is provided in (12).

Propositions 3 and 5 present generalized expressions of the conditional Laplace transform of the interference I and the conditional local delay in mobile networks⁴ given a transmission distance. (11) and (12) are corresponding lower and upper bounds, respectively, since the network realizations endure maximum temporal correlation in the static case and are mutually independent in the infinitely mobile case.

To demonstrate the impact of even a very low level of mobility, we calculate the slope of $D_v(\theta | R)$ at $a = 0$. Under UMM, for example, the sensitivity of $D_v(\theta | R)$ at $a_0 = 0$ is given by

$$\frac{\partial D_v(\theta | R)}{\partial a_0} \Big|_{a_0=0} = -\infty.$$

This shows that the local delay decreases drastically with small excursions from the interferers since the uncertainty induced by mobility greatly reduces the temporal correlation of the interference. An identical result also holds for NMM. Figure 2 shows the local delay as a function of the mean speed \bar{v} under UMM and NMM. The simulation curves and upper bounds show the results for the intermediate mobility regime between the static case and the infinitely mobile case. Random mobility of the interferers positively affects the network performance (in terms of the local delay). Long local delays are due to the high temporal correlation of the interference and thus outage, and the random mobility reduces such correlation [3]. The more uncertainty the mobility induces, the less correlated the outage. Therefore, fewer transmission attempts are necessary. Both lower and upper bounds in (11) and (12) get tight as the mean speed \bar{v} increases.

⁴Recall that mobility models only apply to interferers in this section.

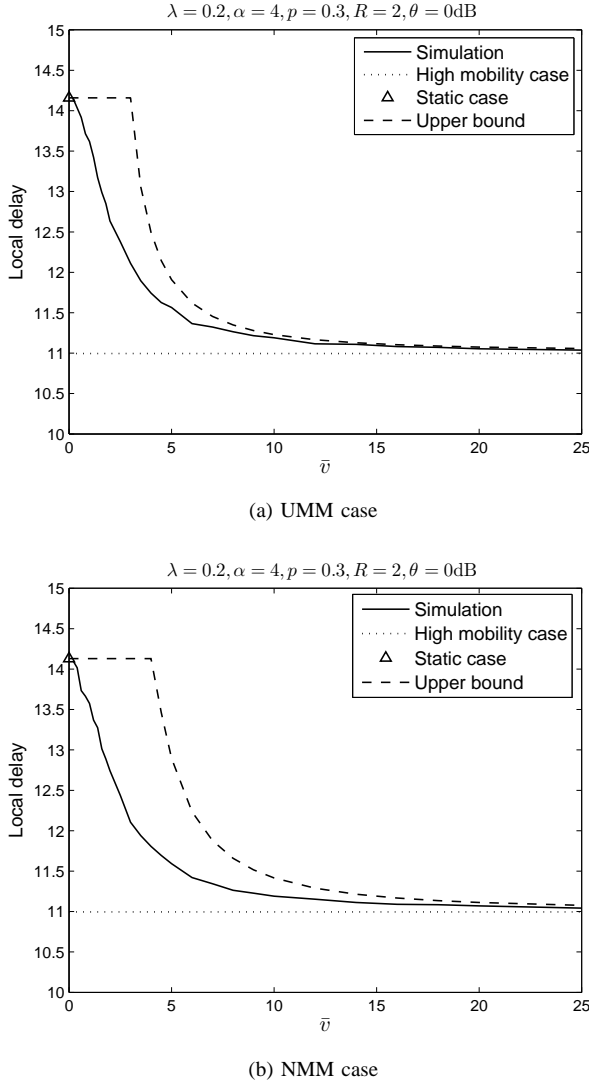


Figure 2: The conditional local delay $D_v(\theta | R)$ as a function of the mean speed \bar{v} under UMM and NMM. $\bar{v} = 128a_0/45\pi$ for UMM and $\bar{v} = \sqrt{\pi}\sigma$ for NMM. The simulation result is the solid curve. The dashed curve is an upper bound from (12). The dotted line is the infinitely mobile case, which provides a lower bound. The static case ($v = 0$) is represented in a triangle.

B. Block mobility

In the previous analysis we assumed fast mobility, where nodes update locations in every time slot. However, this may not be an appropriate assumption for all networks. In a heavy-traffic network, for example, a large number of packets are transferred before a node makes a significant location change. Another example is a mobile network with low speed. In these cases, it is reasonable to use the block mobility model, which includes dwell slots. A node updates its location with probability $1/K$, where $K > 1$, and stays in its previous location with probability $1 - 1/K$. K is the *average location coherence time*. The multi-path fading component, however, is i.i.d. in different time slots. Again, slotted ALOHA is assumed as the MAC scheme.

For any time $t \in \mathbb{Z}$, we partition the transmitter process Φ_t into two PPPs,

$$\Phi_{t,1} = \{x_i(t) \in \Phi_t : x_i(t) \neq x_i(t-1)\}$$

and

$$\Phi_{t,2} = \{x_i(t) \in \Phi_t : x_i(t) = x_i(t-1)\}.$$

The nodes in $\Phi_{t,1}$ update their locations in time t while the nodes in $\Phi_{t,2}$ do not move. $\Phi_{t,1}$ and $\Phi_{t,2}$ are independent with intensities λ/K and $\lambda(K-1)/K$, respectively, due to the independent thinning of the PPP. The total interference is then given by

$$\begin{aligned} I(t) &= \sum_{x \in \Phi_{t,1}} T_x h_x \|x(t)\|^{-\alpha} + \sum_{x \in \Phi_{t,2}} T_x h_x \|x(t)\|^{-\alpha} \\ &= \sum_{y \in \tilde{\Phi}_1} T_y h_y \|y + w_y(t)\|^{-\alpha} + \sum_{x \in \Phi_{t,2}} T_x h_x \|x(t)\|^{-\alpha}, \end{aligned}$$

where $\tilde{\Phi}_1$ is the home location process of the nodes in $\Phi_{t,1}$. In this case, the static elements \mathcal{S} in the network are $\mathcal{S} = \tilde{\Phi}_1 \cup \Phi_2$. We have the following corollary about the conditional Laplace transform of the interference I and the conditional local delay for a given R under the block mobility case.

Corollary 6. *Given the static elements of a network $\mathcal{S} = \tilde{\Phi}_1 \cup \Phi_2$, where $\tilde{\Phi}_1$ and Φ_2 are independent, the conditional Laplace transform of the interference $I(t)$ is given by*

$$\mathcal{L}_I(s | \mathcal{S}) = \mathcal{L}_v(s | \tilde{\Phi}_1) \mathcal{L}_0(s | \Phi_2), \quad (15)$$

where $\mathcal{L}_v(\cdot)$ and $\mathcal{L}_0(\cdot)$ are from (9) and (7), respectively. Let $a = a_0$ under UMM and $a = \sqrt{2}\sigma$ under NMM. Given the transmission distance R , the conditional local delay is upper bounded by

$$D_K(\theta | R) \leq \begin{cases} D_0(\theta | R) \cdot \exp\left(\frac{\lambda p \gamma R^2}{K} \left(\frac{\pi a^2}{\pi a^2 - p \gamma R^2} - \frac{1}{q^{1-\delta}}\right)\right) & a\beta > R \\ D_0(\theta | R) & \text{otherwise,} \end{cases} \quad (16)$$

where the spatial contention γ is from (14), $\beta \triangleq \sqrt{(1-q^{1-\delta})\pi/p\gamma}$, and $D_0(\theta | R)$ is from (13).

Proof: $\mathcal{L}_I(s | \mathcal{S})$ in (15) is straightforward due to the independence property of $\tilde{\Phi}_1$ and Φ_2 . For the local delay, we have

$$D_K(\theta | R) = \frac{1}{p} \mathbb{E}_{\tilde{\Phi}_1} \left(\frac{1}{\mathcal{L}_I(s | \tilde{\Phi}_1)} \right) \mathbb{E}_{\Phi_2} \left(\frac{1}{\mathcal{L}_I(s | \Phi_2)} \right) \Big|_{s=\theta R^\alpha}.$$

The rest of the steps follow the proofs of (10) and (12) in Propositions 3 and 5, respectively. ■

Figure 3 shows the local delay as a function of the mean location coherence time K under both UMM and NMM. The mean speed in the simulations is set at $\bar{v} = 7/K$. The mean speed decreases with the increase of the mean coherence time K , since the average hop length of nodes (if the node moves) is kept constant. The mean coherence time K greatly affects the local delay in the low K regime, while its impact shrinks in the high K regime. (16) provides a tight upper bound and thus can be used to approximate the intermediate results between the static and fast mobility cases. For the case where the dwell time is a constant, the local delay can be analyzed through similar steps.

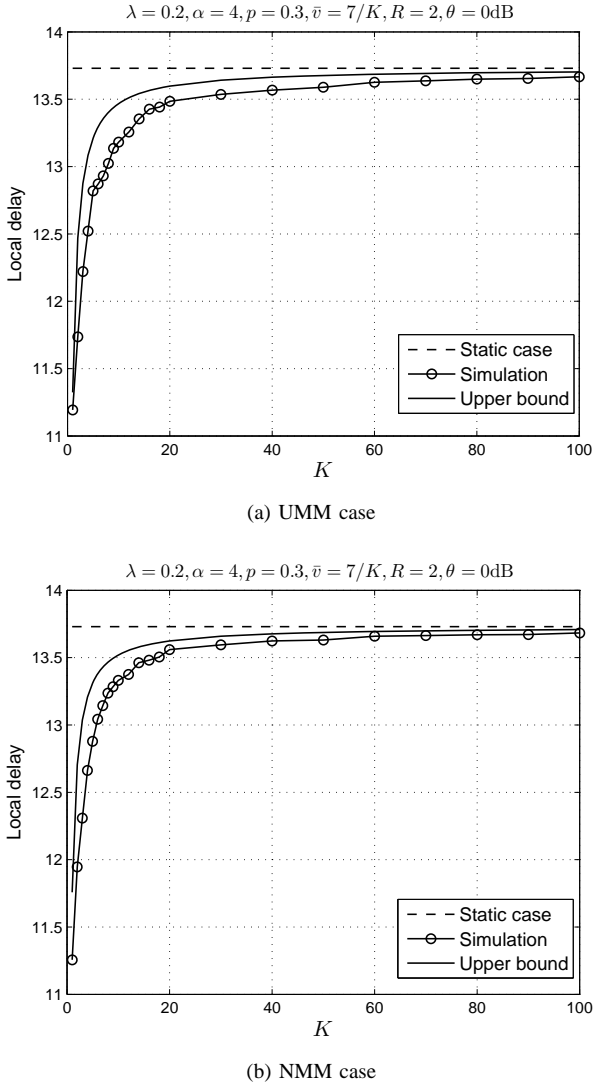


Figure 3: The conditional local delay $D_K(\theta | R)$ as a function of the mean location coherence time K under UMM and NMM. The simulation and an upper bound from (16) are marked by circles and solid curve, respectively. The dashed line is the static case.

IV. LOCAL DELAY FOR RANDOM STATIC TRANSMISSION DISTANCE

In the previous section, we evaluated the local delay for a given transmission distance R . If R itself is a random variable, we can average over the random distance by

$$D_v = \mathbb{E}_R [D_v(\theta | R)].$$

Note that we still do not consider mobility in the desired link (mobility models only apply to the interferers). The randomness of R is due to the spatial averaging over different network realizations. In the rest of the paper, we assume fast mobility at the interferers. Block mobility ($K > 1$) can be treated similarly by replacing $D_v(\theta | R)$ by $D_K(\theta | R)$. As already defined in Section II-E, the desired receiver is located at the origin o . If the location of the desired transmitter is uniformly distributed, we have the following proposition about the local delay.

Proposition 7. Assume that the desired transmitter is uniformly distributed around o with radius a_0 so that R is distributed as given in (2), and the interferers follow UMM. The local delay for $\beta = \sqrt{(1 - q^{1-\delta})\pi/p\gamma} < 1$ is upper bounded by

$$D_{\text{FMOI},a_0} \leq \frac{\pi}{\gamma p^2} \left(1 - q^{1-\delta} e^{\bar{c}_u} (q^{\delta-1} - 1) \right) + \frac{\pi \bar{c}_u e^{-\bar{c}_u}}{\gamma p^2} \left(\text{Ei}(\bar{c}_u q^{\delta-1}) - \text{Ei}(\bar{c}_u) \right) + \frac{\pi q^{1-\delta}}{\gamma \bar{c}_u p^2} \left(e^{\frac{\bar{c}_u p \gamma}{\pi q^{1-\delta}}} - e^{\bar{c}_u} (q^{\delta-1} - 1) \right), \quad (17)$$

where $\text{Ei}(x) \triangleq \int_{-\infty}^x t^{-1} e^t dt$, $\bar{c}_u \triangleq \lambda \pi a_0^2$ is the mean number of nodes in a circular region of radius a_0 , and ‘‘FMOI’’ is the abbreviation of ‘‘fast mobility only at interferers’’.

For $\beta \geq 1$, the local delay is upper bounded by

$$D_{\text{FMOI},a_0} \leq \frac{\pi}{\gamma p^2} \left(1 - \left(1 - \frac{p\gamma}{\pi} \right) e^{\frac{\bar{c}_u p \gamma}{\pi - p\gamma}} + \bar{c}_u e^{-\bar{c}_u} \left(\text{Ei} \left(\frac{\pi \bar{c}_u}{\pi - p\gamma} \right) - \text{Ei}(\bar{c}_u) \right) \right). \quad (18)$$

The local delay is lower bounded by

$$D_{\text{FMOI},a_0} \geq \frac{\pi}{\gamma \bar{c}_u p^2} \left(e^{\frac{\bar{c}_u p \gamma}{\pi}} - 1 \right). \quad (19)$$

Proof: See Appendix II. \blacksquare

Similarly we have the following proposition, if the location of the desired transmitter is normally distributed.

Proposition 8. Assume that the desired transmitter is normally distributed around o with parameter σ so that the distribution of R is given in (4), and the interferers follow NMM. Let $\beta = \sqrt{(1 - q^{1-\delta})\pi/p\gamma}$. The local delay is upper bounded by

$$D_{\text{FMOI},\sigma} < \frac{\pi}{\gamma p^2} \exp \left((q^{1-\delta} - 1) \left(\frac{\pi}{p\gamma} - \bar{c}_n q^{\delta-1} \right) \right) \cdot \left(1 - q^{1-\delta} + \frac{p\gamma}{\pi - p\gamma \bar{c}_n q^{\delta-1}} \right), \quad (20)$$

if $2\sigma^2 < q^{1-\delta}/\lambda p\gamma$, where $\bar{c}_n \triangleq 2\lambda \pi \sigma^2$, and lower bounded by

$$D_{\text{FMOI},\sigma} \geq \frac{\pi}{p(\pi - \bar{c}_n p\gamma)}, \quad (21)$$

if $2\sigma^2 < 1/\lambda p\gamma$. The local delay is infinite for $2\sigma^2 > q^{1-\delta}/\lambda p\gamma$.

Proof: See Appendix III. \blacksquare

The local delay is always finite if the location of the desired transmitter is uniformly distributed, since the support of transmission distance R is finite. Figure 4 corroborates the observation. This observation can be extended to any pdf of R via Proposition 5 as long as it has finite support. If the location of the desired transmitter is normally distributed, however, the local delay is finite only if $2\sigma^2 < q^{1-\delta}/\lambda p\gamma$. If the randomness of the transmission distance induces too much uncertainty in the typical link, the local delay becomes heavy-tailed. The infinity of the local delay does not imply that a node can not convey a message to other nodes in the network

in a finite time. However, it implies that the distribution of the local delay is heavy-tailed.

The next proposition contrasts the local delay for mobility only at interferers with the result for static networks.

Proposition 9. *If the location of the desired transmitter is uniformly distributed, the local delay in a static network is given by*

$$D_{\text{static},a_0} = \frac{\pi q^{1-\delta}}{\bar{c}_u \gamma p^2} \left[\exp\left(\frac{\bar{c}_u p \gamma}{\pi q^{1-\delta}}\right) - 1 \right]. \quad (22)$$

If the location of the desired transmitter is normally distributed, the local delay is finite if $2\sigma^2 < q^{1-\delta}/\lambda p \gamma$ and given by

$$D_{\text{static},\sigma} = \frac{\pi q^{1-\delta}}{p(\pi q^{1-\delta} - \bar{c}_n p \gamma)}. \quad (23)$$

Proof: In a static network, the static elements in the network are $\mathcal{S} = \Phi$. Given a transmission distance R , the local delay is given by $D_0(\theta | R)$, which is from (13). Deconditioning on the random variable R in (13) using (2), we have

$$D_{\text{static},a_0} = \int_0^{a_0} \frac{2r}{a_0^2} D_0(\theta | r) dr,$$

which yields (22). Similarly for the Rayleigh pdf of R given in (4), we have

$$D_{\text{static},\sigma} = \int_0^\infty \frac{r}{p\sigma^2} \exp\left(\frac{\lambda p \gamma r^2}{q^{1-\delta}} - \frac{r^2}{2\sigma^2}\right) dr.$$

The integral is finite if $2\sigma^2 < q^{1-\delta}/\lambda p \gamma$. (23) then follows from straightforward calculations. ■

We denote by $\bar{D}_{\text{FMOI},a_0}$ and $\bar{D}_{\text{FMOI},\sigma}$ the upper bounds of the local delay given in Proposition 7 and 8, respectively. We then have the following corollary.

Corollary 10. *For $a_0 \rightarrow \infty$, $\bar{D}_{\text{FMOI},a_0}$ and D_{static,a_0} have the following relationship*

$$\bar{D}_{\text{FMOI},a_0} = \begin{cases} \Theta(D_{\text{static},a_0}) & \beta < 1 \\ o(D_{\text{static},a_0}) & \beta \geq 1. \end{cases} \quad (24)$$

For $\sigma = \sqrt{\frac{q^{1-\delta}}{2\lambda p \gamma}}$, we have

$$\frac{\bar{D}_{\text{FMOI},\sigma}}{D_{\text{static},\sigma}} \Big|_{\sigma = \sqrt{\frac{q^{1-\delta}}{2\lambda p \gamma}}} = 1. \quad (25)$$

Proof: See Appendix IV. ■

We define $\bar{R} \triangleq \mathbb{E}[R]$ as the mean transmission distance. Figures 4 shows the local delay as a function of \bar{R} for both $\beta < 1$ and $\beta \geq 1$. We find that mobility at the interferers helps reduce the local delay. However, the local delay is dominantly affected by the distribution of the transmission distance.

V. LOCAL DELAY FOR RANDOM TIME-VARIANT TRANSMISSION DISTANCE

In this section, we evaluate the local delay under several transmission schemes. Conditioned on $o \in \tilde{\Phi}$, the success probability given the static element \mathcal{S} is given by

$$\mathbb{P}^o(\mathcal{C}_S) = \mathbb{P}^o(\text{SIR} > \theta | \mathcal{S}),$$

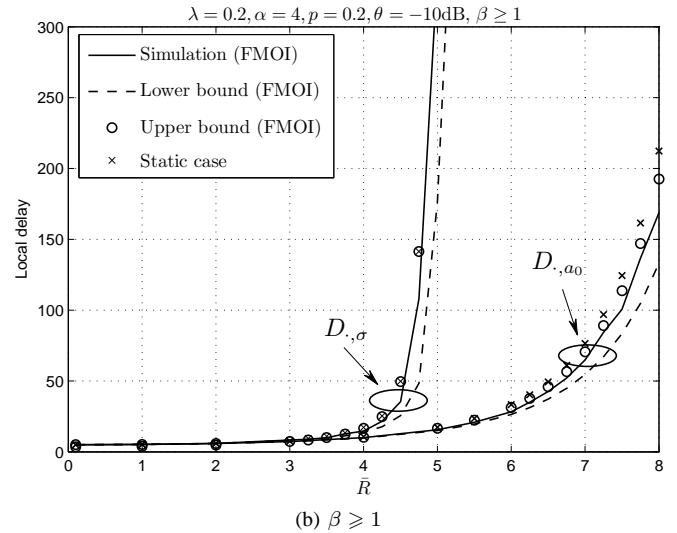
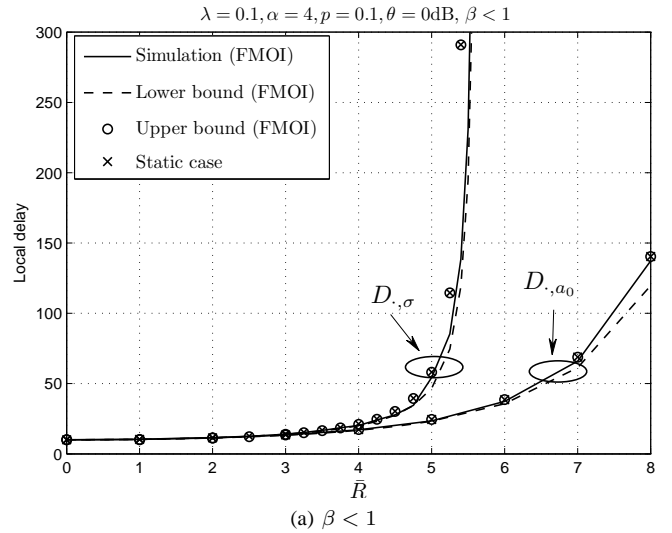


Figure 4: The local delay as a function of the mean transmission distance $\bar{R} = \mathbb{E}[R]$, where $a_0 = 45\pi\bar{R}/128$ and $\sigma = \bar{R}/\sqrt{\pi}$. The solid curve shows the simulation results for fast mobility only at interferers with their upper and lower bounds in circles and dashed lines, respectively. The crosses are the static case.

where $\mathbb{P}^o(\cdot)$ is the Palm distribution [17]. The local delay is then given by

$$D \triangleq \mathbb{E}_S^o \left(\frac{1}{\mathbb{P}^o(\mathcal{C}_S)} \right).$$

A. Random bipolar model

Here, we evaluate the local delay under the random bipolar model, which is described in Section II-B. It is complicated to analyze the case of fast mobility in both desired and interfering links directly. Hence we consider a joint random variable $G \triangleq hR^{-\alpha}$, since the macroscopic mobility in wireless networks can be treated as another source of uncertainty in addition to multipath fading [3], [21]. Given the static elements in the network $\mathcal{S} = \tilde{\Phi}$, the conditional success probability is

$$\mathbb{P}^o(G > \theta I(t) | \tilde{\Phi}) = \mathbb{E}_G \left[\mathbb{P}^o \left(I(t) < \theta^{-1} G | G, \tilde{\Phi} \right) \right].$$

In order to evaluate the local delay, we need the following lemma.

Lemma 11. *For a static network (the static elements in the network $\mathcal{S} = \Phi$), we have the following relationship of the conditional success probability*

$$\mathbb{E}_G [\mathbb{P}^o (I(t) < \theta^{-1}G | G, \Phi)] \geq \mathbb{P}^o (I(t) < \theta^{-1}\mathbb{E}[G] | \Phi). \quad (26)$$

Proof: See Appendix V. ■

Deconditioning on the point process leads to the following proposition.

Proposition 12. *The local delay under the random bipolar model is always finite, i.e.,*

$$D_v = \mathbb{E}_\Phi^o \left[\frac{1}{p\mathbb{E}_G [\mathbb{P}^o (I(t) < \theta^{-1}G | G, \tilde{\Phi})]} \right] < \infty.$$

Proof: The local delay under the random bipolar model is given by

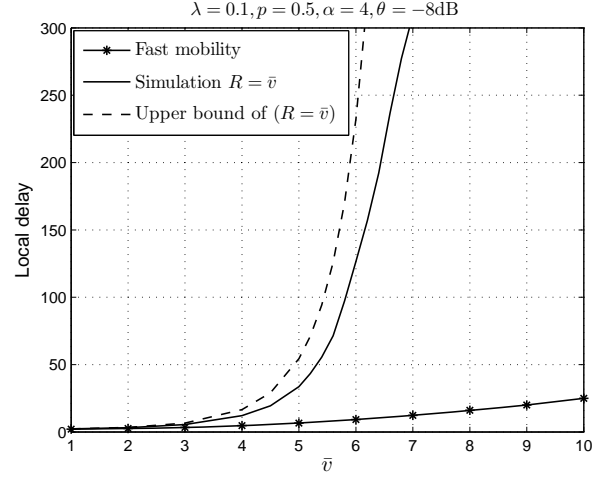
$$\begin{aligned} & \mathbb{E}_\Phi^o \left[\frac{1}{p\mathbb{E}_G [\mathbb{P}^o (I(t) < \theta^{-1}G | G, \tilde{\Phi})]} \right] \\ & \leq \mathbb{E}_\Phi^o \left[\frac{1}{p\mathbb{E}_G [\mathbb{P}^o (I(t) < \theta^{-1}G | G, \Phi)]} \right] \\ & \stackrel{(a)}{\leq} \mathbb{E}_\Phi^o \left[\frac{1}{p\mathbb{P}^o (I(t) < \theta^{-1}\mathbb{E}[G] | \Phi)} \right] \\ & < \infty, \end{aligned}$$

where (a) holds due to Lemma 11. ■

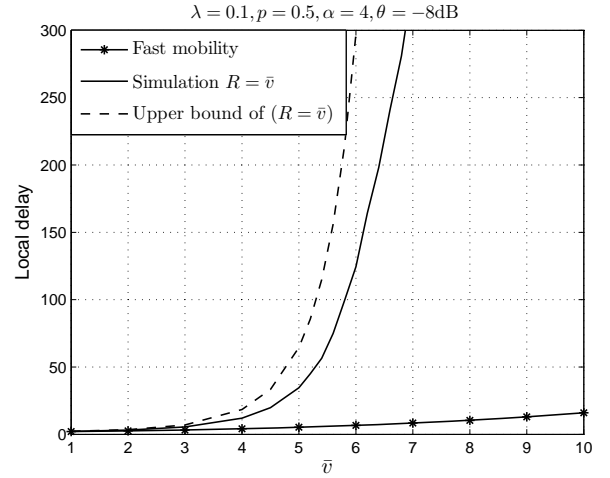
The simulation results under the fast mobility case are shown in Figure 5. For comparison, we also show the conditional local delay for a given transmission distance R , where $R = \bar{v}$. The benefit of fast mobility is obvious from the figure, since the nodes take advantage of spatial diversity in the desired link and mobility reduces the temporal correlation of interference in the interfering links. We notice from the figures that the local delay increases with the mean speed \bar{v} . This is because the long transmission distance more than offsets the benefit of the spatial diversity of the desired transmitter. An alternative way is to let a transmitter talk to the receiver that is close to it, as explored in the next subsection.

B. Quasi-nearest-receiver (QNR) transmission

Here, we assume that each transmitter tries to talk to its quasi-nearest receiver whose home location is the closest to the receiver. We only discuss UMM. Recall from Section II-B2 that the potential receiver process Ψ is a PPP with intensity $\lambda' = q\lambda$. The assumption maintains the same density of receivers as the nodes that are not scheduled for transmission. Ψ is independent of the transmitter process Φ_t . We assume the typical transmitter has its home location at the origin o and denote by R_0 the distance between the home location of the transmitter to its quasi-nearest receiver. To calculate the local delay under the quasi-nearest-receiver transmission, we need the following lemma.



(a) UMM case



(b) NMM case

Figure 5: Local delay under the random bipolar model for UMM and NMM. For comparison, the conditional local delay for a fixed transmission distance $R = \bar{v}$ is also included, where the upper bound is from (12) with $R = \bar{v}$.

Lemma 13. *Let R_0 denote the distance between the home location of the typical transmitter to its quasi-nearest receiver and a_0 denote the radius of the mobility region of the transmitter. Given R_0 , upper and lower bounds of the local delay under the quasi-nearest-receiver transmission are given by $D_v(r_{\max})$ and $D_\infty(r_{\min})$, where $r_{\max} = R_0 + a_0$ and $r_{\min} = \max\{0, R_0 - a_0\}$.*

Proof: The lemma is proved by evaluating the local delay at two extreme points in the mobility region. ■

Based on the Rayleigh distribution of R_0 obtained in [22], we have the following proposition.

Proposition 14. *A lower bound of the local delay under quasi-nearest-receiver transmission is given by*

$$\begin{aligned} \underline{D}_{\text{QNR}} &= \frac{1}{p} (1 - e^{-q\bar{c}_u}) - \frac{2\pi q\lambda}{p} \exp\left(\frac{pq\gamma\bar{c}_u}{q\pi - p\gamma}\right) \\ & \phi\left(a_0, \frac{a_0 p\gamma}{q\pi - p\gamma}, \frac{p\gamma - q\pi}{\pi}\right), \end{aligned} \quad (27)$$

if $p < \pi / (\pi + \gamma)$, where

$$\begin{aligned} \phi(x, m, s) &= \int_x^\infty t \exp(s(t+m)^2) dt, \\ &= m \sqrt{\frac{\pi}{-s}} \left(\frac{1}{2} \operatorname{erf} \left(\frac{x}{\sqrt{2\sigma^2}} - \frac{1}{2} \right) \right) - \\ &\quad \frac{1}{2s} \exp(s(x+m)^2), \quad s < 0. \end{aligned} \quad (28)$$

For $\beta \leq 1$, an upper bound of the local delay is given by

$$\begin{aligned} \bar{D}_{\text{QNR}} &= \frac{2\pi q\lambda}{p} \exp\left(\frac{pq\gamma\bar{c}_u}{q^{2-\delta}\pi - p\gamma}\right) \cdot \\ &\quad \phi\left(0, \frac{p\gamma a_0}{p\gamma - q^{2-\delta}\pi}, \frac{\lambda(p\gamma - q^{2-\delta}\pi)}{q^{1-\delta}}\right), \end{aligned} \quad (29)$$

if $q^{2-\delta}/p > \gamma/\pi$, where $\phi(x, m, s)$ is from (28).

For $\beta > 1$, we have an upper bound

$$\begin{aligned} \bar{D}_{\text{QNR}} &= \frac{1}{p} \int_0^{(\beta-1)a_0} \varphi(x) dx + \\ &\quad \frac{2\pi q\lambda}{p} \exp\left(\frac{pq\gamma\bar{c}_u}{q^{2-\delta}\pi - p\gamma}\right) \cdot \\ &\quad \phi\left((\beta-1)a_0, \frac{p\gamma a_0}{p\gamma - q^{2-\delta}\pi}, \frac{\lambda(p\gamma - q^{2-\delta}\pi)}{q^{1-\delta}}\right), \end{aligned} \quad (30)$$

if $q^{2-\delta}/p > \gamma/\pi$, where

$$\varphi(x) = f_{R_0}(x) \exp\left(\frac{p\gamma\bar{c}_u(x+a_0)^2}{a_0^2\pi - p\gamma(x+a_0)^2}\right) \quad (31)$$

and $f_{R_0}(x) = 2\pi q\lambda x e^{-\pi q\lambda x^2}$.

Proof: From Lemma 13, a lower bound of the local delay is

$$\underline{D}_{\text{QNR}} = \frac{1}{p} \int_0^{a_0} f_{R_0}(x) dx + \int_{a_0}^\infty f_{R_0}(x) D_\infty(x-a_0) dx.$$

The integral is finite if $p < \pi / (\pi + \gamma)$. On the other hand, an upper bound of the local delay is given by

$$\bar{D}_{\text{QNR}} = \int_0^\infty f_{R_0}(x) D_v(x+a_0) dx.$$

The integral is finite if $q^{2-\delta}/p > \gamma/\pi$. The rest of the calculation is straightforward. ■

Figure 6 shows the local delay as a function of the MAC parameter p in mobile networks under quasi-nearest-receiver transmission. For comparison, the local delay in static networks is also included. From the figure, we observe that fast mobility reduces the local delay (compared to the static case), but it helps little to keep the local delay finite. This is due to the fact that the mobility induces limited diversity under the quasi-nearest-receiver transmission. For other transmission schemes such as quasi-nearest-neighbor transmission etc., we can calculate bounds of the local delay in similar ways.

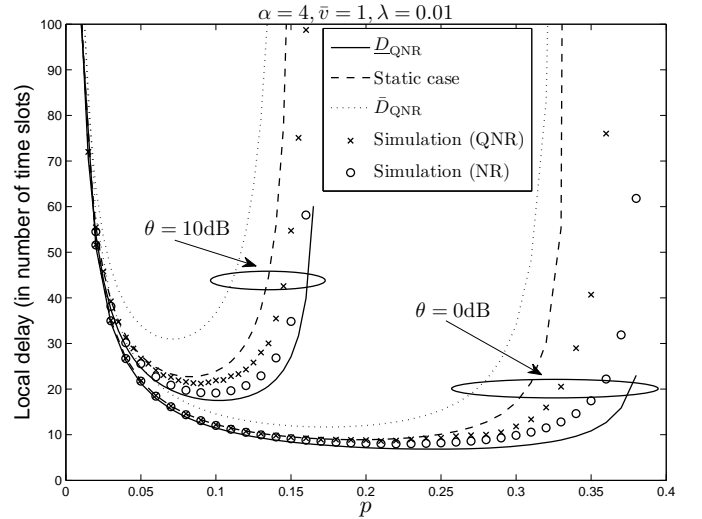


Figure 6: The local delay as a function of the transmission probability p under quasi-nearest-receiver and nearest-receiver transmission schemes. The crosses and circles are the simulation results of QNR and NR schemes, respectively. The dotted line is an upper bound of the local delay under the QNR scheme (see (29) and (30)). The dashed line is the static case from [2, (24)]. The solid curve is a lower bound of the local delay under the QNR scheme (see (27)).

C. Nearest-receiver (NR) transmission

If each transmitter always tries to talk its nearest receiver, we have the following proposition about the local delay.

Proposition 15. *The local delay under nearest-receiver transmission D_{NR} is lower and upper bounded by*

$$\underline{D}_{\text{QNR}} \leq D_{\text{NR}} \leq \bar{D}_{\text{QNR}}, \quad (32)$$

where $\underline{D}_{\text{QNR}}$ is from (27).

Proof: Conditioned on that the quasi-nearest receiver of the typical transmitter is at $(R_0, 0)$, there are no other receivers in the ball of $B(o, R_0)$, where the origin o is the center of the ball and R_0 is the radius. Hence, even if the typical transmitter always chooses its nearest receiver, the transmission distance is not less than $r_{\min} = \max\{R_0 - a_0, 0\}$, where a_0 is the mobility radius of the transmitter. D_{NR} is then lower bounded by $\underline{D}_{\text{QNR}}$. On the other hand, the typical transmitter changes the destination in different time t , if there is another receiver that is closer to the transmitter than the quasi-nearest receiver when the transmitter moves. The spatial correlation of the interference at different receivers is (much) lower. Hence, the local delay under nearest-receiver transmission is upper bounded by \bar{D}_{QNR} . ■

Figure 6 shows the simulation results of the local delay under nearest-receiver transmission, which corroborates Proposition 15.

VI. CONCLUSIONS

In this paper, we have evaluated the local delay in mobile Poisson networks for deterministic, random static, and random time-variant transmission distance. The results provide generalized expressions in addition to the two previously explored cases of static and infinitely mobile networks. Fast mobility has been shown to reduce the local delay in Poisson

networks since the mobility of the interferers decreases the spatio-temporal correlation of the interference and outage, and mobility from the desired transmitter induces spatial diversity during transmission. The uniform and normal mobility models as specific examples lead to quantitatively different local delay, even if the mean speeds of the nodes under two models are at an identical level. The range of network parameters under which a finite local delay can be achieved has also been derived, which depends on different mobility models and transmission schemes. Furthermore, the frequency with which the nodes make significant changes in locations greatly affects the local delay performance. The more frequently the nodes update their location, the fewer attempts a transmitter needs for packet transmission.

APPENDIX I

Here, we present the proof of Proposition 5. We first prove a general (looser) upper bound that $D_v(\theta | R) \leq D_0(\theta | R)$. Since

$$\int_{\mathbb{R}^2} \frac{f_w(x)}{\|y+x\|^\alpha + \theta R^\alpha} dx \leq \frac{1}{\|y\|^\alpha + \theta R^\alpha},$$

we have

$$\begin{aligned} D_v(\theta | R) &\leq \lim_{a \rightarrow 0} \mathbb{E}_{\tilde{\Phi}} \left(\frac{1}{p\mathcal{L}_I(\theta | \tilde{\Phi})} \right) \\ &= \frac{1}{p} \exp \left(\frac{\delta\pi^2 p \lambda \theta^\delta R^2}{q^{1-\delta} \sin(\pi\delta)} \right) = D_0(\theta | R). \end{aligned}$$

Next we prove a tighter upper bound for large a ($a = a_0$ under UMM, and $a = \sqrt{2}\sigma$ under NMM). We first consider UMM. From (1) and (10), we have

$$\begin{aligned} D_v(\theta | R) &= \frac{1}{p} \exp \left(\lambda \int_{\mathbb{R}^2} \left(\frac{1}{1 - p\theta R^\alpha \int_{\mathbb{R}^2} \frac{f_w(z-y)}{\|z\|^\alpha + \theta R^\alpha} dz} - 1 \right) dy \right) \\ &= \frac{1}{p} \exp \left(\lambda \int_{B(0, a_0)} \left(\frac{1}{1 - \frac{p\theta R^\alpha}{\pi a_0^2} \int_{B(y, a_0)} \frac{1}{\|z\|^\alpha + \theta R^\alpha} dz} - 1 \right) dy \right) \\ &\quad \exp \left(\lambda \int_{\mathbb{R}^2 \setminus B(0, a_0)} \left(\frac{1}{1 - \frac{p\theta R^\alpha}{\pi a_0^2} \int_{B(y, a_0)} \frac{1}{\|z\|^\alpha + \theta R^\alpha} dz} - 1 \right) dy \right) \end{aligned} \quad (33)$$

$$\stackrel{(a)}{\leq} \frac{1}{p} \exp \left(\lambda \int_{B(0, a_0)} \left(\frac{1}{1 - \frac{p\theta R^\alpha}{\pi a_0^2} \int_{\mathbb{R}^2} \frac{1}{\|z\|^\alpha + \theta R^\alpha} dz} - 1 \right) dy \right), \quad a_0 > R\sqrt{\frac{p\gamma}{\pi}} \quad (34)$$

$$= \frac{1}{p} \exp \left(\frac{\lambda \pi a_0^2 p \gamma R^2}{\pi a_0^2 - p \gamma R^2} \right), \quad a_0 > R\sqrt{\frac{p\gamma}{\pi}}, \quad (35)$$

where (a) holds when $a_0 > R\sqrt{p\gamma/\pi}$ due to the fact that $o \notin \lim_{a_0 \rightarrow \infty} B(ca_0, a_0)$ for any $c > 1$; the second exponential component in (33) hence goes to 0 for large a_0 . On the other hand, we have another upper bound $D_v(\theta | R) \leq D_0(\theta | R)$. Taking the minimum of (35) and $D_0(\theta | R)$ yields (12), since $\pi a^2(1 - q^{1-\delta}) > p\gamma R^2$ implies that $\pi a^2 > p\gamma R^2$.

For NMM, we have

$$\begin{aligned} D_v(\theta | R) &= \frac{1}{p} \exp \left(\lambda \int_{\mathbb{R}^2} \left(\frac{1}{1 - \frac{p\theta R^\alpha}{2\pi\sigma^2} \int_{\mathbb{R}^2} \frac{\exp(-\|z-y\|^2/2\sigma^2)}{\|z\|^\alpha + \theta R^\alpha} dz} - 1 \right) dy \right) \\ &\stackrel{(a)}{\leq} \frac{1}{p} \exp \left(\lambda \int_{\mathbb{R}^2} \left(\frac{1}{1 - \frac{p\theta R^\alpha}{2\pi\sigma^2} \int_{B(y, \sqrt{2}\sigma)} \frac{1}{\|z\|^\alpha + \theta R^\alpha} dz} - 1 \right) dy \right) \\ &\stackrel{(b)}{\leq} \frac{1}{p} \exp \left(\frac{2\lambda\pi\sigma^2 p \gamma R^2}{2\pi\sigma^2 - p\gamma R^2} \right), \quad \sigma > R\sqrt{\frac{p\gamma}{2\pi}}, \end{aligned} \quad (36)$$

where (a) holds since the non-negative function $1/(\|x\|^\alpha + \theta)$ is monotonically decreasing with the increase of $\|x\|$, the fact that the indicator function $\mathbf{1}(\|x\| \leq \sqrt{2}\sigma) \geq \exp(-\|x\|^2/2\sigma^2)$ for $\forall x \in B(0, \sqrt{2}\sigma)$, and $\int_{\mathbb{R}^2} \mathbf{1}(\|x\| \leq \sqrt{2}\sigma) dx = \int_{\mathbb{R}^2} \exp(-\|x\|^2/2\sigma^2) dx$; (b) follows from the proof of (35).

APPENDIX II

Here, we present the proof of Proposition 7. For a given transmission distance R , an upper bound of the conditional local delay $D_v(\theta | R)$ is given in (12). If the location of the desired transmitter is uniformly distributed, we obtain

$$\begin{aligned} D_{\text{FMOI}, a_0} &\leq \int_0^{a_0} f_R(r) D_v(\theta | r) dr \\ &= \begin{cases} \frac{1}{pa_0^2} \int_0^{\beta^2 a_0^2} \exp\left(\frac{\bar{c}_n x}{\pi a_0^2 - p\gamma x}\right) dx + \\ \frac{1}{a_0^2} \int_{\beta a_0}^{a_0} 2x D_0(\theta x^\alpha) dx & \beta < 1 \\ \frac{1}{pa_0^2} \int_0^{a_0^2} \exp\left(\frac{\bar{c}_n x}{\pi a_0^2 - p\gamma x}\right) dx & \beta \geq 1, \end{cases} \end{aligned}$$

where $f_R(r)$ is from (2). On the other hand,

$$D_{\text{FMOI}, a_0} \geq \int_0^{a_0} f_R(r) D_\infty(\theta | r) dr,$$

where $D_\infty(\theta | r)$ is from (11). The rest of the steps are straightforward.

APPENDIX III

Here, we present the proof of Proposition 8. Similar to the proof of Proposition 7, the local delay is lower bounded by

$$D_{\text{FMOI}, \sigma} \geq \int_0^\infty \frac{1}{2\sigma^2 p} \exp\left(-\frac{x}{2\sigma^2} + \lambda p \gamma x\right) dx.$$

The integral is bounded if $2\sigma^2 < 1/\lambda p \gamma$. On the other hand, the local delay is upper bounded by

$$\begin{aligned} D_{\text{FMOI}, \sigma} &\leq \int_0^{2\beta^2\sigma^2} \frac{1}{2\sigma^2 p} \exp\left(-\frac{x}{2\sigma^2} + \frac{\bar{c}_n p \gamma x}{2\pi\sigma^2 - p\gamma x}\right) dx + \\ &\quad \int_{2\beta^2\sigma^2}^\infty \frac{1}{2\sigma^2 p} \exp\left(-\frac{x}{2\sigma^2} + \frac{\lambda p \gamma x}{q^{1-\delta}}\right) dx \\ &\stackrel{(a)}{=} \frac{\pi \exp\left((q^{1-\delta} - 1) \left(\frac{\pi}{p\gamma} - \bar{c}_n q^{\delta-1}\right)\right)}{p(\pi - p\gamma \bar{c}_n q^{\delta-1})} + \\ &\quad \frac{\exp\left(-\frac{\pi}{p\gamma} - \bar{c}_n\right) \int_{2\pi\sigma^2/p\gamma}^{2\pi\sigma^2/p\gamma} \exp\left(\frac{x}{2\sigma^2} + \frac{2\bar{c}_n \sigma^2 \pi}{p\gamma x}\right) dx, \end{aligned}$$

where (a) holds when $2\sigma^2 < q^{1-\delta}/\lambda p\gamma$. For small σ , we obtain

$$\begin{aligned} & \int_{2\pi\sigma^2 q^{1-\delta}/p\gamma}^{2\pi\sigma^2/p\gamma} \exp\left(\frac{x}{2\sigma^2} + \frac{2\pi\sigma^2\bar{c}_n}{p\gamma x}\right) dx \\ & \approx \frac{2\pi\sigma^2}{p\gamma} (1 - q^{1-\delta}) \exp\left(\frac{\pi q^{1-\delta}}{p\gamma} + \bar{c}_n q^{\delta-1}\right). \end{aligned}$$

APPENDIX IV

Here, we present the proof of Corollary 10. Based on (22), it is straightforward to find that for $a_0 \rightarrow \infty$,

$$D_{\text{static},a_0} = \Theta\left(\frac{\exp\left(\frac{\bar{c}_u p\gamma}{\pi q^{1-\delta}}\right)}{\bar{c}_u}\right).$$

For $\beta < 1$, \bar{D}_{FMOI} is given in (17). We have

$$\begin{aligned} \lim_{a_0 \rightarrow \infty} \frac{\bar{D}_{\text{FMOI},a_0} \bar{c}_u}{\exp\left(\frac{\bar{c}_u p\gamma}{\pi q^{1-\delta}}\right)} & \stackrel{(a)}{=} \lim_{a \rightarrow \infty} \frac{\bar{c}_u^2 \int_{\bar{c}_u}^{\bar{c}_u q^{\delta-1}} \exp(t)/t dt}{\exp\left(\frac{\bar{c}_u(\pi q^{1-\delta} + p\gamma)}{\pi q^{1-\delta}}\right)} + \frac{\pi q^{1-\delta}}{\gamma p^2} \\ & \stackrel{(b)}{=} \frac{\pi q^{1-\delta}}{\gamma p^2} < \infty, \end{aligned}$$

where (a) and (b) hold due to L'Hopital's rule and the fact that $\beta = \sqrt{(1 - q^{1-\delta})\pi/p\gamma} < 1$. Hence, we have

$$\bar{D}_{\text{FMOI},a_0} = \Theta(D_{\text{static},a_0}), \quad \beta < 1.$$

For $\beta > 1$, on the other hand, \bar{D}_{FMOI} is given in (18). It is straightforward to show that

$$\lim_{a_0 \rightarrow \infty} \frac{\bar{D}_{\text{FMOI},a_0} \bar{c}_u}{\exp\left(\frac{p\gamma\bar{c}_u}{\pi q^{1-\delta}}\right)} = 0.$$

For $\beta = 1$, we have

$$\begin{aligned} & \lim_{a_0 \rightarrow \infty} \frac{\bar{D}_{\text{FMOI},a_0} \bar{c}_u}{\exp\left(\frac{\bar{c}_u p\gamma}{\pi q^{1-\delta}}\right)} \\ & = \lim_{a_0 \rightarrow \infty} \frac{\pi \bar{c}_u \int_{\bar{c}_u}^{\pi \bar{c}_u / (\pi - p\gamma)} \exp(t)/t dt}{\gamma p^2 \exp(\bar{c}_u(\pi q^{1-\delta} + p\gamma)/\pi q^{1-\delta})} - \\ & \quad \lim_{a_0 \rightarrow \infty} \left(1 - \frac{p\gamma}{\pi}\right) \frac{\pi \bar{c}_u}{\gamma p^2} \\ & \stackrel{(a)}{=} 0, \end{aligned}$$

where (a) holds due to the fact that $\pi - p\gamma = \pi q^{1-\delta}$. (24) is then proved.

For $\sigma = \sqrt{q^{1-\delta}/2\lambda p\gamma}$, (25) is immediate from (20) and (23) via L'Hopital's rule.

APPENDIX V

Here, we present the proof of Lemma 11. We have

$$\begin{aligned} & \frac{\partial^2}{\partial G^2} \mathbb{P}^\sigma(I(t) < \theta^{-1}G \mid G, \Phi) \\ & = \frac{\partial^2}{\partial G^2} \prod_{x \in \Phi} \left(1 - \frac{p\theta^{-1}G}{\|x\|^\alpha + G\theta^{-1}}\right) \\ & = \frac{\partial}{\partial G} \sum_{x_i \in \Phi} \left(-\frac{p\theta^{-1}\|x_i\|^\alpha}{(\|x_i\|^\alpha + G\theta^{-1})^2} \prod_{x \in \Phi, x \neq x_i} \left(1 - \frac{p\theta^{-1}G}{\|x\|^\alpha + G\theta^{-1}}\right)\right) \\ & = \sum_{x_i \in \Phi} \left(\frac{2p\theta^{-1}\|x_i\|^\alpha}{(\|x_i\|^\alpha + G\theta^{-1})^3} \prod_{x \in \Phi, x \neq x_i} \left(1 - \frac{p\theta^{-1}G}{\|x\|^\alpha + G\theta^{-1}}\right)\right) + \\ & \quad \sum_{x_i \in \Phi} \sum_{x_j \in \Phi, x_j \neq x_i} \left(\prod_{x \in \{x_i, x_j\}} \frac{p\theta^{-1}\|x\|^\alpha}{(\|x\|^\alpha + G\theta^{-1})^2}\right) \cdot \\ & \quad \prod_{x \in \Phi \setminus \{x_i, x_j\}} \left(1 - \frac{p\theta^{-1}G}{\|x\|^\alpha + G\theta^{-1}}\right) \\ & \geq 0. \end{aligned}$$

Hence (26) holds due to Jensen's inequality.

REFERENCES

- [1] F. Baccelli and B. Blaszczyszyn, "A New Phase Transition for Local Delays in MANETs," in *IEEE INFOCOM'10*, (San Diego, CA), Mar. 2010.
- [2] M. Haenggi, "The Local Delay in Poisson Networks," *IEEE Transactions on Information Theory*, 2012. Accepted. Available at <http://www.nd.edu/~mhaenggi/pubs/tit12.pdf>.
- [3] Z. Gong and M. Haenggi, "Interference and Outage in Mobile Random Networks: Expectation, Distribution, and Correlation," *IEEE Transactions on Mobile Computing*, Accepted, 2012. Available at <http://www.nd.edu/~mhaenggi/pubs/tmc13.pdf>.
- [4] G. Alfano, R. Tresch, and M. Guillaud, "Spatial diversity impact on the local delay of homogeneous and clustered wireless networks," in *Smart Antennas (WSA), 2011 International ITG Workshop on*, pp. 1–6, IEEE, 2011.
- [5] X. Zhang and M. Haenggi, "Random Power Control in Poisson Networks," *IEEE Transactions on Communications*, vol. 60, pp. 2602–2611, Sept. 2012.
- [6] K. Gulati, R. K. Ganti, J. G. Andrews, B. L. Evans, and S. Srikanteswara, "Characterizing decentralized wireless networks with temporal correlation in the low outage regime," *IEEE Transactions on Wireless Communications*, vol. 11, pp. 3112–3125, Aug. 2012.
- [7] M. J. Neely and E. Modiano, "Capacity and Delay Tradeoffs for Ad Hoc Mobile Networks," vol. 51, no. 6, pp. 1917–1937, 2005.
- [8] R. Vaze, "Throughput-delay-reliability tradeoff with ARQ in wireless ad hoc networks," *IEEE Transactions on Wireless Communications*, vol. 10, no. 7, pp. 2142–2149, 2011.
- [9] M. J. Neely, "Optimal energy and delay tradeoffs for multi-user wireless downlinks," *IEEE Transaction on Information Theory*, vol. 53, pp. 3095–3113, Sept 2007.
- [10] J. Liu, X. Jiang, H. Nishiyama, and N. Kato, "Delay and capacity in ad hoc mobile networks with f-cast relay algorithms," *IEEE Transactions on Wireless Communications*, vol. 10, no. 8, pp. 2738–2751, 2011.
- [11] L. Dai, "Stability and delay analysis of buffered aloha networks," *IEEE Transactions on Wireless Communications*, vol. 11, no. 8, pp. 2707–2719, 2012.
- [12] C. Bettstetter, "Mobility modeling in wireless networks: categorization, smooth movement, and border effects," *ACM SIGMOBILE Mobile Computing and Communications Review*, vol. 5, no. 3, p. 66, 2001.
- [13] Z. Kong and E. M. Yeh, "On the latency for information dissemination in mobile wireless networks," in *Proceedings of the 9th ACM International Symposium on Mobile Ad Hoc Networking and Computing (MobHoc)*, Hong Kong SAR, China, May 2008.
- [14] C. Bettstetter, "On the connectivity of ad hoc networks," *The Computer Journal*, vol. 47, no. 4, p. 432, 2004.

- [15] Y. Peres, A. Sinclair, P. Sousi, and A. Stauffer, "Mobile geometric graphs: detection, coverage and percolation," in *Proceedings of the Twenty-Second Annual ACM-SIAM Symposium on Discrete Algorithms*, pp. 412–428, SIAM, 2011.
- [16] M. Grossglauser and D. N. C. Tse, "Mobility increases the capacity of ad hoc wireless networks," *IEEE/ACM Transactions on Networking*, vol. 10, no. 4, pp. 477–486, 2002.
- [17] M. Haenggi, *Stochastic Geometry for Wireless Networks*. Cambridge University Press, 2012.
- [18] E. Hyttia, P. Lassila, and J. Virtamo, "Spatial node distribution of the random waypoint mobility model with applications," *IEEE Transactions on Mobile Computing*, vol. 5, no. 6, pp. 680–694, 2006.
- [19] J. Kingman, "Uses of exchangeability," *The Annals of Probability*, pp. 183–197, 1978.
- [20] F. Baccelli, *Stochastic Geometry and Wireless Networks. Volume II-Applications*. Foundations and Trends in Networking (NOW Publishers), vol. 4, no. 1-2, pp. 1-312, 2009.
- [21] M. Haenggi, "A Geometric Interpretation of Fading in Wireless Networks: Theory and Applications," *IEEE Transactions on Information Theory*, vol. 54, pp. 5500–5510, Dec 2008.
- [22] M. Haenggi, "On Distances in Uniformly Random Networks," *IEEE Transactions on Information Theory*, vol. 51, pp. 3584–3586, Oct. 2005.